J|A|C|S
ARTICLES
Published on Web 04/17/2002

Radial Control of Recognition and Redox Processes with Multivalent Nanoparticle Hosts

Andrew K. Boal and Vincent M. Rotello*

Contribution from the Department of Chemistry, University of Massachusetts, Amherst, Massachusetts 01003

Received August 20, 2001

Abstract: Mixed Monolayer Protected Gold Clusters (MMPCs) featuring both hydrogen bonding and aromatic stacking molecular recognition functionalities have been used to create multivalent hosts for flavins. Multitopic binding of these hosts to flavin was shown to have a strong radial dependence: when the recognition site was brought closer to the MMPC surface, recognition was enhanced ~3-fold due to increased preorganization. The effect of preorganization is reversed upon reduction of flavin, where the MMPC with longer side chains bind the flavin guest ~7-fold stronger than the short chain counterpart due to unfavorable dipolar interactions between the electron-rich aromatic stacking units of the host and the anionic flavin guest. This fine-tuning of recognition and redox processes provides both a model for enzymatic systems and a tool for the fabrication of devices.

Introduction.

Tuning of cofactor reduction potentials through redox-state dependent interactions is central to the function of redox enzymes. For example, flavoproteins use specific interactions such as hydrogen bonding, aromatic stacking, and dipolar effects to regulate the recognition, and hence redox potential of the flavin cofactor in various oxidation states.[1] Preorganization of the flavin binding site in these enzymes is determined through a complex pattern of intraprotein and protein−cofactor interactions provided by the protein matrix. The degree of preorganization of the active site plays an important role in controlling cofactor redox processes,[2] variably enhancing favorable and enforcing unfavorable protein−cofactor interactions in different cofactor redox states.[3]

Effective models and mimics of enzymatic systems enhance our understanding of these complex systems.[4,5] Moreover, redox enzymes provide prototypes for the creation of devices: biomimetic redox modulation of recognition processes allows access to molecular devices such as shuttles[6] and switches.[7] Conversely, recognition-mediated control of redox processes provides a tool for the creation of molecular scale electronic devices.[8,5c]

While there have been a number of systems made to explore mono- and multivalent redox-dependent host−guest interactions,[9] the ability to tune recognition and redox properties through control of preorganization remains an important challenge.[10] Mixed Monolayer Protected Gold Clusters (MMPCs)[11] bearing molecular recognition elements in the monolayer[12,13] are a potential tool for creating tunable receptors for model systems[14] and device applications.[15] The monolayer coatings of MMPCs are radial in nature: order decreases with increasing distance from the gold core.[16] This effect has been probed earlier

* Corresponding author. E-mail: rotello@chem.umass.edu.

(1) Fraaije, M. W.; Mattevi, A. *Trends Biochem. Sci.* **2000**, *25*, 126−132. For an extensive discussion of flavoenzyme structure and function, see: *Chemistry and Biochemistry of Flavoenzymes*; Müller, F., Ed.; CRC: Boca Raton, FL, 1991; Vols. 1−3.
(2) Kasim, M.; Swenson, R. P. *Biochemistry* **2000**, *39*, 15322−15332.
(3) (a) Anthony, C. *Biochem. J.* **1996**, *320*, 697−711. (b) Ghisla, S.; Massey, V. *Eur. J. Biochem.* **1989**, *181*, 1−17. (c) Popov, V.; Lamzin, V. S. *Biochem. J.* **1994**, *301*, 625−643. (d) Blakley, R. L.; Benkovic, S. J. *Chemistry and Biochemistry of Pterins*; Wiley: New York, 1985.
(4) For a recent example of the synergy between biochemical studies and model systems of flavoenzymes, see: Bradley, L. H.; Swenson, R. P. *Biochemistry* **2001**, *40*, 8686−8695. Cuello, A. O.; McIntosh, C. M.; Rotello, V. M. *J. Am. Chem. Soc.* **2000**, *122*, 3517−3521
(5) (a) Kirby, A. J. *Acc. Chem. Res.* **1997**, *30*, 290−296. (b) Riley, D. P. *Acc. Chem. Res.* **1999**, *32*, 2573−2588. (c) Niemz, A.; Rotello, V. M. *Acc. Chem. Res.* **1999**, *32*, 44−52. (d) Gust, D.; Moore, T. A.; Moore, A. L. *Acc. Chem. Res.* **2001**, *34*, 40−48. (e) Hasford, J.; Kemnitzer, W.; Rizzo, C. *J. Org. Chem.* **1997**, *62*, 5244−5245.
(6) Anelli, P. L.; Spencer, N.; Stoddart, J. F. *J. Am. Chem. Soc.* **1991**, *113*, 5131−5132.
(7) Otsuki, J.; Tsujino, M.; Iizaki, T.; Araki, K.; Seno, M.; Takatera, K.; Watanabe, T. *J. Am. Chem. Soc.* **1997**, *119*, 7895−7896.
(8) Pease, A. R.; Jeppesen, J. O.; Stoddart, J. F.; Luo, Y.; Collier, C. P.; Heath, J. R. *Acc. Chem. Res.* **2001**, *43*, 433−444.
(9) See, inter alia: (a) Kaifer, A. E. *Acc. Chem. Res.* **1999**, *32*, 62−71. (b) Yano, Y. *Rev. Heteroatom Chem.* **2000**, *22*, 151−179.
(10) (a) Fernandez-Saiz, M.; Schneider, H.-J.; Sartorius, J.; Wilson, D. W. *J. Am. Chem. Soc.* **1996**, *118*, 4739−4745. (b) Hettich, R.; Schneider, H.-J. *J. Am. Chem. Soc.* **1997**, *119*, 5638−5647.
(11) (a) Brust, M.; Walker, M.; Bethell, D.; Schiffrin, D. J.; Whymann, R. *J. Chem. Soc., Chem. Commun.* **1994**, 801−802. (b) Hostetler, M. J.; Templeton, A. C.; Murray, R. W. *Langmuir* **1999**, *15*, 3782−3789.
(12) For a recognition study in a planar SAM, see: Motesharei, K.; Myles, D. C. *J. Am. Chem. Soc.* **1998**, *120*, 7328−7336.
(13) For a flavoenzyme model study using a planar SAM, see: Tam-Chang, S.-W.; Mason, J.; Iverson, I.; Hwang, K.-O.; Leonard C. *J. Chem. Soc., Chem. Commun.* **1999**, 65−66.
(14) (a) Boal, A. K.; Rotello, V. M. *J. Am. Chem. Soc.* **1999**, *121*, 4941−4942. (b) Boal, A. K.; Rotello, V. M. *J. Am. Chem. Soc.* **2000**, *122*, 734−735.
(15) (a) Shipway, A. M.; Willner, I. *Acc. Chem. Res.* **2001**, *34*, 421−432. (b) Liu, J.; Xu, R.; Kaifer, A. E. *Langmuir* **1998**, *14*, 7337−7339. (c) Aherne, D.; Rao, S. N.; Fitzmaurice, D. *J. Phys. Chem. B* **1999**, *103*, 1821−1825. (d) Fitzmaurice, D.; Rao, S. N.; Preece, J. A.; Stoddart, J. F.; Wenger, S.; Zaccheroni, N. *Angew. Chem., Int. Ed. Engl.* **1999**, *38*, 1147−1150. (e) Liu, J.; Alvarez, J.; Kaifer, A. E. *Adv. Mater.* **2000**, *12*, 1381−1383. (f) Labande, A.; Astruc, D. *Chem. Commun.* **2000**, 1007−1008. (g) Kim, Y.; Johnson, R. C.; Hupp, J. T. *Nano Lett.* **2001**, *1*, 165−167.
(16) (a) Luedtke, W. D.; Landman, U. *J. Phys. Chem.* **1996**, *100*, 13323−13329. (b) Hostetler, M. J.; Stokes, J. J.; Murray, R. W. *Langmuir* **1996**, *12*, 3604−3612.

10.1021/ja016894k CCC: $22.00

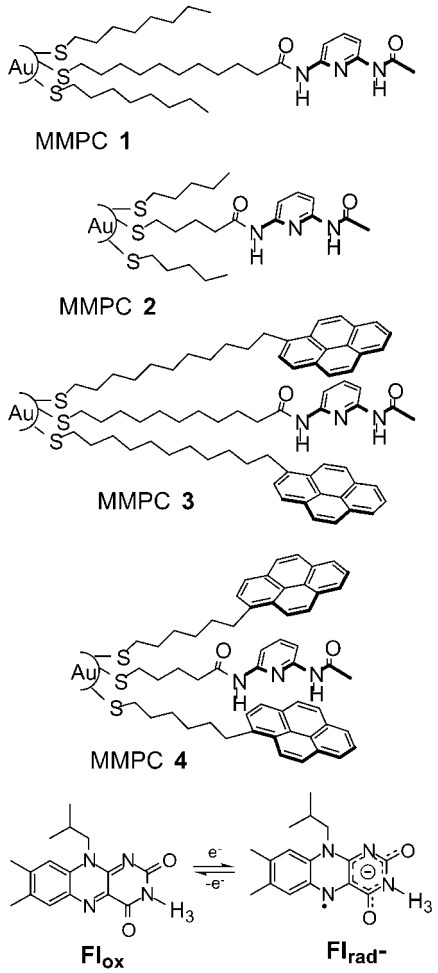

Figure 1. MMPCs **1**−**4** and flavin **Fl**.

by us in a study of *intra*monolayer hydrogen bonding in MMPCs, where a steady decrease in hydrogen bonding efficiency was observed.[17] We report here the extension of this radial control to the redox-specific multivalent recognition of a flavin guest.

Results and Discussion

To provide a series of MMPCs for quantifying the effect of chain length on mono- and ditopic recognition of flavin **Fl**, MMPCs **1**−**4** were prepared (Figure 1). In this family, MMPCs **1** and **2** are functionalized with only hydrogen-bonding elements (diaminopyridine) while MMPCs **3** and **4** contain both hydrogen-bonding and aromatic stacking (pyrene) elements. Comparison of MMPCs **1** and **2** featuring monotopic recognition sites with ditopic MMPC receptors **3** and **4** respectively then allows direct quantification of the effects of multitopic interaction. For all MMPCs, the core size was ∼1.5 nm in diameter.[18] Monolayer composition was determined using NMR endgroup analysis. The monolayers for MMPCs **1**−**4** contained approximately 12, 8, 12, and 11 diaminopyridine recognition sites (of a total of ∼90 total ligands), respectively.[19]

Recognition of $\mathbf{Fl_{ox}}$ by MMPCs **1**−**4** was quantified through NMR titration in $CDCl_3$. The shifts of the N(3) proton of $\mathbf{Fl_{ox}}$ during sequential addition of each of the hosts were readily fitted to a 1:1 binding isotherm.[20] As expected, there was no difference in the affinity of monotopic receptors **1** and **2** on the recognition of $\mathbf{Fl_{ox}}$ (Table 1). In contrast, there was a large radial effect observed for ditopic MMPC receptors **3** and **4**. With the longer chain length system, ditopic receptor **3** binds $\mathbf{Fl_{ox}}$ ∼2-fold more strongly than the corresponding monotopic receptor **1**. A much stronger enhancement in recognition is observed with shorter chain length, with ditopic receptor **4** binding $\mathbf{Fl_{ox}}$ ∼5-fold more strongly than monotopic receptor **2**. The greater contribution of aromatic stacking to binding in the shorter chain length MMPC **4** is a direct outcome of the increased preorganization of this system.[21]

Table 1. Binding Constants and Reduction Potentials for MMPC−Fl Complexes

MMPC	$K_a(\mathbf{Fl_{ox}})$ (M^{-1})[a]	ΔG_a (kcal/mol)	$\Delta E_{1/2}$ (mV)[a]	$K_a(\mathbf{Fl_{rad}}^-)$ (M^{-1})[a]	ΔG_a (kcal/mol)
1	196 ± 8[b]	−3.09	+86[b]	6400 ± 1100	−5.1
2	185 ± 11	−3.06	+75	3900 ± 800	−4.8
3	320 ± 20[c]	−3.38	+49	2300 ± 400	−4.5
4	930 ± 47	−4.01	−26	<320	<−3.4

[a] At 296 K, all $E_{1/2}$ values are ±5 mV. Uncertainties for $K_a(\mathbf{Fl_{ox}})$ were obtained from the standard error of the titration curve fit. Uncertainties for $K_a(\mathbf{Fl_{rad}}^-)$ were based upon the uncertainty of $K_a(\mathbf{Fl_{ox}})$ coupled with a ±5 mV uncertainty in the $E_{1/2}$. [b] Values from ref 14a. [c] From ref 14b.

To further quantify radial control over multivalent binding of MMPC hosts **1**−**4** on **Fl**, the reduction potential of **Fl** in the presence of these hosts was measured using Square Wave Voltammetry (SWV) (Figure 2). Addition of MMPCs **1** and **2** made the potential of the $\mathbf{Fl_{ox}}$−$\mathbf{Fl_{rad}}^-$ reduction substantially less negative due to the hydrogen bond-mediated stabilization of $\mathbf{Fl_{rad}}^-$ (Table 1).[5c] As was observed for binding of $\mathbf{Fl_{ox}}$ by monotopic receptors **1** and **2**, there was no appreciable effect of chain length on the observed reduction potential of **Fl**. Ditopic receptors **3** and **4**, however, had strikingly different effects on the reduction potential of **Fl**, with the longer chain length MMPC **3** making the reduction potential less negative and the shorter chain length MMPC **4** making this potential *more* negative.

The differing effects of MMPCs **1**−**4** on the reduction potential of **Fl** can be understood by comparing the binding of these receptors to $\mathbf{Fl_{ox}}$ and $\mathbf{Fl_{rad}}^-$. The binding constants of MMPCs **1**−**4** with $\mathbf{Fl_{rad}}^-$ provided in Table 1 were obtained through the relation:

$$\frac{K_a(\text{red})}{K_a(\text{ox})} = e^{(nF/RT)(E_{1/2}(\text{bound})-E_{1/2}(\text{unbound}))} \quad (1)$$

A summary of association constants of both $\mathbf{Fl_{ox}}$ and $\mathbf{Fl_{rad}}^-$ to MMPC hosts **1**−**4** is given in Figure 3.[22] As expected from the increase in electron density at the imide carbonyls that occurs

(17) Boal, A. K.; Rotello, V. M. *Langmuir* **2000**, *16*, 9527−9532.
(18) Determined from UV−vis spectra, see: Duff, D. G.; Baiker, A.; Edwards, P. P. *J. Chem. Soc., Chem. Commun.* **1993**, 96−97.
(19) See: Ingram, R. S.; Hostetler, M. J.; Murray, R. W. *J. Am. Chem. Soc.* **1997**, *119*, 9175−9178.
(20) See Supporting Information for titration plots.
(21) The increase in recognition observed for the diaminopyridine−pyrene systems arising from multivalent recognition indicates the absence of extensive phase segregation in these systems.
(22) Application of Formula (1) requires an accurate measurement of $E_{1/2}$ (bound). With the slow scan rates used in this experiment, the degree of binding observed during the reduction process is determined by the higher affinity process (i.e. $\mathbf{Fl_{rad}}^-$ binding by MMPCs **1**−**3**, and $\mathbf{Fl_{ox}}$ by MMPC **4**). By this measure, >90% complexation is predicted for each of the host−guest dyads except MMPC **4** (where we can only obtain an upper limit for the calculated affinity). For further examples of complexation at relatively low host concentrations, see: Rotello, V. M. In *Molecular Recognition and Inclusion*; Coleman, A., Ed.; Kluwer: Amsterdam, The Netherlands, 1998; pp 479−482.

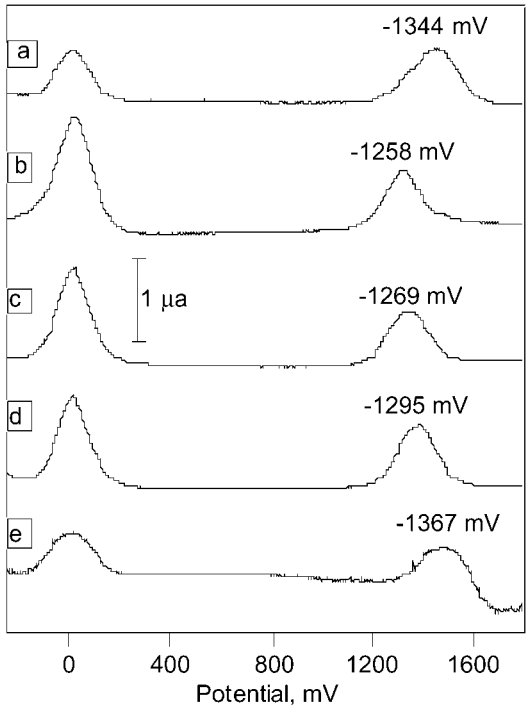

Figure 2. Square wave voltammograms of **Fl** (a) alone and with (b) MMPC **1**, (c) MMPC **2**, (d) MMPC **3**, and (e) MMPC **4**. Voltammograms were recorded under the following conditions: [**Fl**] = 0.05 mM (0.025 mM for d); 100 equiv of MMPC-attached diaminopyridine units; solvent, CH_2Cl_2; supporting electrolyte, 0.1 M Bu_4NClO_4; internal ferrocene reference set to 0 mV potential; scan period, 400 ms; step height, 2 mV; T = 23 °C.

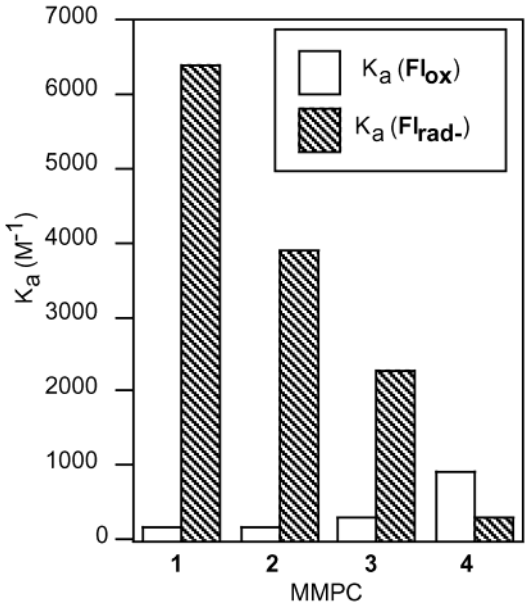

Figure 3. Association constants of Fl_{ox} and Fl_{rad}- to MMPCs **1**−**4**.

upon reduction of the flavin moiety, monotopic MMPCs **1** and **2** show strongly enhanced binding of Fl_{rad}- relative to Fl_{ox}. The affinities of these two systems for Fl_{rad}- are similar, with the longer chain system binding slightly more strongly, most likely due to a slightly greater degree of congestion at the surface of the shorter monolayer.

The ditopic MMPCs **3** and **4** possess opposite selectivities for Fl_{ox} relative to Fl_{rad}-: MMPC **3** preferentially binds Fl_{rad}- while MMPC **4** preferentially binds Fl_{ox}. This inversion in redox state preference can be rationalized by comparison of the

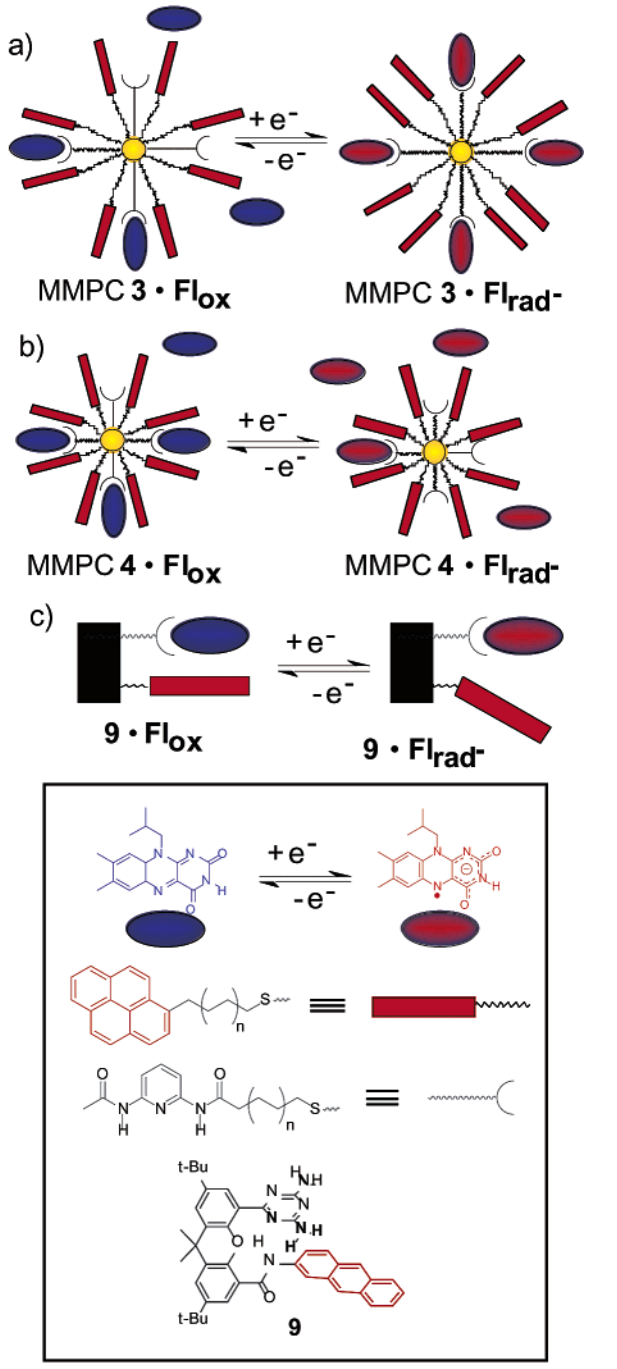

Figure 4. Representation of the expected effects on chain length in redox-modulated binding of Fl_{ox}/Fl_{rad}- to MMPCs with multivalent binding sites (a) far from and (b) close to the nanoparticle surface as well as (c) a small molecular multivalent receptor, **9**.

corresponding mono- and multitopic MMPC receptors. For long side chain MMPC **3**, aromatic stacking increases the affinity for Fl_{ox} by 0.3 kcal/mol, and decreases the affinity for Fl_{rad}- by 0.6 kcal/mol relative to the corresponding MMPC **1**. For the shorter side chain receptors **2** and **4** this effect is magnified, with the aromatic stacking of **4** enhancing binding of Fl_{ox} by 0.95 kcal/mol, and decreasing the binding affinity for Fl_{rad}- by 1.7 kcal/mol. The enhancement in binding of Fl_{ox} by receptors **3** and **4** as compared to hosts **1** and **2** arises from the favorable stacking interaction of the electron-deficient Fl_{ox} with the electron-rich pyrene side chains. Similarly, the decrease in affinity of **3** and **4** with Fl_{rad}- arises from unfavorable interac-

tions between the now electron-rich $\mathbf{Fl_{rad}}$- and the electron-rich pyrene (Figure 4a,b). The differences in these systems are a direct consequence of the alkane chain length used to attach the recognition elements to the nanoparticle surface. For MMPC **3**, which is made with 11 carbon chains, the elements are not tightly packed (Figure 4a). When **Fl** undergoes reduction, the pyrene components can move away from the anion and thus minimize repulsive interactions. This is not possible for MMPC **4**, where the 6 carbon alkane chains translate into a denser monolayer, providing a system that is unable to relieve repulsive stacking interactions (Figure 4b). This enforcement of unfavorable interactions mimics that observed in a number of flavoenzymes,[23] with the preorganization provided by the monolayer serving the same role as that provided by the active site. It should be noted that this behavior was not observed in our previous small molecule multitopic enzyme models, e.g. **9** (Figure 4c).[5c] In these systems, the mobility of the anthracene ring allows it to move away from $\mathbf{Fl_{rad}}$-, thus precluding the ability of the system to enforce repulsive interactions.[24]

Conclusions

In summary, we have demonstrated that the radial structure of MMPC monolayers can be used to tune multivalent recognition of guest molecules. This modulation of recognition arises from the decrease in preorganization that occurs as the attached recognition elements are moved further away from the nanoparticle surface. Extension of this process to redox-active guests provides a biomimetic means of controlling guest redox potential, and concomitantly a tool for regulating redox-state-specific binding of guest systems. The ability to control multivalent molecular recognition processes using monolayer packing to enforce both attractive and repulsive interactions is a unique aspect of functionalized MMPCs, and provides a new tool for the creation of both enzyme models and functional molecule-based materials.

Experimental Section.

General. 2-amino-6-acetylamidopyridine,[25] flavin $\mathbf{Fl_{ox}}$,[26] and MMPCs **1** and **3**[14] were prepared according to literature methods. Toluene and CH_2Cl_2 were distilled over CaH_2 under argon. All reactions were carried out in oven-dried glassware under an atmosphere of argon. ^{1}H NMR spectra were recorded in $CDCl_3$ (purchased from Cambridge Isotope Labs, Inc.) at 200 MHz and referenced internally to TMS at 0.0 ppm. NMR spectra involving colloids were taken in $CDCl_3$ that had been stirred over K_2CO_3 for at least 24 h prior to use since it was found that residual acid sometimes caused rapid decomposition of colloids. All reagents and other solvents were used as received from commercial sources. NMR titrations and electrochemical experiments were run as previously described.[14]

2-*N*-Acetyl-6-*N*-(4-pentenoyl)diaminopyridine (10). 2-Amino-6-acetylamidopyridine (1.9 g, 12.6 mmol) and triethylamine (3.1 g, 25.2 mmol, 4.2 mL) were dissolved in 100 mL of CH_2Cl_2 and cooled to −78 °C in a 250 mL round-bottom flask. 4-Pentenoyl chloride (1.5 g, 12.6 mmol, 1.4 mL) was then added dropwise. The reaction was subsequently stirred overnight at room temperature, during which time it became turbid. The reaction was quenched by the addition of H_2O, washed once with a saturated aqueous NaCl solution, and dried over $MgSO_4$. Solvent removal yielded an orange/brown oily solid, which was purified by column chromatography (SiO_2; EtOAc) to yield the product as a white solid (2.7 g, 92% yield). ^{1}H NMR ($CDCl_3$, 200 MHz) δ (ppm) 7.90, 7.77, 7.69 (d, J = 7.9 Hz; bs; t, J = 7.9 Hz total 5H), 5.58 (m, 1H), 5.07 (m, 2H), 2.48 (m, 4H), 2.18 (s, 3H). IR (thin film from CH_2Cl_2 on NaCl plate) ν_{max} 3280, 3078, 2992, 2935, 1670, 1586, 1510, 1450, 1296, 1232, 1160, 995, 920, 810 cm^{-1}. Anal. Calcd for $C_{12}H_{15}N_3O_2$: C, 61.79; H, 6.48; N, 18.00. Found: C, 61.59; H, 6.48; N, 17.86.

Scheme 1. Synthesis of MMPC **2**

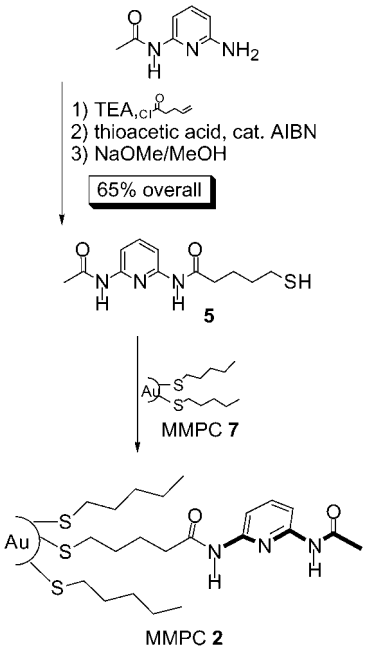

2-*N*-Acetyl-6-*N*-(5-*S*-acetylmercaptopentanoyl)diaminopyridine (11). **10** (2.5 g, 10.7 mmol) was dissolved in 40 mL of toluene in a 100 mL round-bottom flask. Thiolacetic acid (1.67 g, 22 mmol, 1.6 mL) and AIBN (~100 mg) were then added and Ar was bubbled through the solution for 30 min. The solution was then stirred at reflux for 3 h and cooled to room temperature. The reaction was washed once each with saturated aqueous $NaHCO_3$ and NaCl solutions, then dried over $MgSO_4$. Solvent removal yielded a yellow/orange solid, which was purified by column chromatography (SiO_2; EtOAc) to yield the product as a pale yellow solid (2.5 g, 76% yield). ^{1}H NMR ($CDCl_3$, 200 MHz) δ (ppm) 7.88 (d, 2H, J = 8.3 Hz); 7.69 (t, 1H, J = 7.9 Hz), 7.57 (bs, 2H), 2.91 (t, 2H, J = 6.9 Hz), 2.41, 2.34 (m, s, 5H), 2.20 (s, 3H), 1.70 (m, 4H). IR (thin film from CH_2Cl_2 on NaCl plate) ν_{max} 3270, 3080, 2490, 1673, 1589, 1511, 1462, 1303 cm^{-1}. Anal. Calcd for $C_{14}H_{19}N_3O_3S$: C, 54.36; H, 6.19; N, 13.58. Found: C, 54.50; H, 6.15; N, 13.54.

2-*N*-Acetyl-6-*N*-(5-mercaptopentanoyl)diaminopyridine (5). **11** (1.0 g, 3.23 mmol) was dissolved in 20 mL of MeOH in a 50 mL round-bottom flask. The clear solution was next purged for 20 min with Ar, followed by the addition of NaOMe (0.6 g, 7.0 mmol, 1.5 mL of a 30 wt % solution in MeOH) followed with an additional 10 min of Ar purge. The reaction was then allowed to stir overnight, and was quenched by the addition of excess saturated aqueous NH_4Cl and removal of the methanol. The resulting slurry was then dissolved in EtOAc and washed twice with H_2O and once with saturated aqueous NaCl and dried over $MgSO_4$. Solvent removal yielded a light yellow solid, which was purified by column chromatography (SiO_2; 1:1 EtOAc: hexanes) to yield the product as a white solid (800 mg, 92% yield). ^{1}H

(23) (a) Ludwig, M. L.; Luschinsky, C. L. In *Chemistry and Biochemistry of Flavoenzymes*; Mueller, F., Ed.; CRC Press: Boca Raton, FL, 1990; Vol. 3, pp 427−466. (b) Swenson, R.; Krey, G.; Eren, M. In *Flavins and Flavoproteins*; Edmondson, D., McKormick, D., Eds.; de Gruyter: Berlin, Germany, 1987; pp 98−107.
(24) For a system where aromatic stacking was enforced through covalent and hydrophobic forces, see: Seward E. M.; Hopkins R. B.; Sauerer W.; Tam S. W.; Diederich F. *J. Am. Chem. Soc.* **1990**, *112*, 1783−1790
(25) Bernstein, J.; Stearns, B.; Shaw, E.; Lott, W, A. *J. Am. Chem. Soc.* **1947**, *69*, 1151−1154.
(26) Breinlinger, E.; Niemz, A.; Rotello, V. M. *J. Am. Chem. Soc.* **1995**, *117*, 5379−5380.

NMR ($CDCl_3$, 200 MHz) δ (ppm) 7.89 (d, 2H, J = 8.4 Hz), 7.70 (t, 1H, J = 7.8 Hz), 2.57 (q, 2H, J = 6.9 Hz), 2.40 (t, 2H, J = 7.4 Hz), 2.20 (s, 3H), 1.56 (m, 4H), 1.38 (t, 1H, J = 7.9 Hz). IR (thin film from CH_2Cl_2 on NaCl plate) ν_{max} 3275, 3081, 2928, 2875, 1675, 1591, 1511, 1423, 1305 cm^{-1}. Anal. Calcd for $C_{12}H_{18}N_3O_2S$: C, 53.72; H, 6.76; N, 15.66. Found: C, 53.90; H, 6.65; N, 15.55.

MMPC 7. $HAuCl_4 \cdot 3H_2O$ (250 mg, 0.64 mmol) was dissolved in 150 mL of deionized H_2O in a 500 mL round-bottom flask to give a golden yellow solution. Tetra-*n*-octylammonium bromide (700 mg, 1.3 mmol) and 150 mL of toluene were then added and the mixture was stirred. After 15 min, the organic layer had become dark red and the aqueous phase colorless. Pentanethiol (80 mg, 0.77 mmol, 0.1 mL) was then added, causing the organic phase to become turbid orange. $NaBH_4$ (260 mg, 5 mmol) was then added dropwise as a solution in 5 mL of H_2O, causing an immediate color change to dark brown and the evolution of gas. After 3 h, the organic phase was collected and the solvent removed. The resulting residue was dissolved in ca. 20 mL of toluene and 200 mL of EtOH was added to precipitate the colloid. When precipitation was complete, the product was collected by filtration and washed multiple times with EtOH to fully remove unreacted thiol. ^1H NMR ($CDCl_3$, 200 MHz) δ (ppm) 1.55 (bs), 1.25 (bs), 0.88 (bs). IR (thin film from CH_2Cl_2 on NaCl plate) ν_{max} 2915, 2890, 1485, 1320 cm^{-1}. UV−vis (CH_2Cl_2 solution) λ_{max} 230, 290, 495 (shoulder) nm.

MMPC 2. MMPC **7** (500 mg) and **5** (90 mg, 0.34 mmol) were dissolved in 40 mL of CH_2Cl_2 in a 100 mL round-bottom flask. The resulting dark brown solution was purged with Ar for 30 min., then allowed to stir for 2 days under Ar. The CH_2Cl_2 was removed, and the resulting brown solid was stirred for several hours as a suspension in CH_3CN and filtered. This process was repeated as necessary, typically twice, to completely remove unbound thiols as detected by either TLC or NMR. ^1H NMR ($CDCl_3$, 200 MHz) δ (ppm) 7.89 (bs, 1H), 0.5−2.5 (mbs, 29H). IR (thin film from CH_2Cl_2 on NaCl plate) ν_{max} 3320, 2995, 2910, 2885, 1630, 1520, 1485, 1310 cm^{-1}. UV−vis (CH_2Cl_2 solution) λ_{max} 234, 292, 500 (shoulder) nm.

5-Bromopentane-1-pyrene ketone (**12**). 6-Bromohexanoic acid (5.3 g, 27 mmol) was dissolved in 40 mL of CH_2Cl_2 in a 100 mL round-bottom flask. Oxalyl chloride (3.4 g, 27 mmol, 2.4 mL) was added, followed by a drop of DMF, and an immediate evolution of gas was observed. This reaction was allowed to stir until gas evolution stopped, approximately 1 h. The solution of the acid chloride was then transferred to a second, 250 mL round-bottom flask containing pyrene (5.0 g, 24.7 mmol) and $AlCl_3$ (4.0 g, 30 mmol) in 40 mL of CH_2Cl_2 that had been cooled to −78 °C. Upon addition of the acid chloride, the originally deep red solution became dark green. The reaction was allowed to stir for 3 h at −78 °C, and then quenched by the careful addition of 1 M aqueous HCl. The deep yellow reaction mixture was then washed once with aqueous NaCl and dried over $MgSO_4$. Solvent removal gave the crude product as a yellow-orange paste that was purified by column chromatography (SiO_2; 1:9 CH_2Cl_2:hexanes) to yield the product as an off-white solid (4.2 g, 47% yield). ^1H NMR ($CDCl_3$, 200 MHz) δ (ppm) 8.88 (d, 1H, J = 9.38 Hz), 8.03−8.36 (m, 8H), 3.46 (t, 2H, J = 6.9 Hz), 3.26 (t, 2H, J = 7.6 Hz), 1.97 (m, 4H), 1.66 9m, 2H). IR (thin film from CH_2Cl_2 on NaCl plate) ν_{max} 3042, 2950, 1692, 1248, 875 cm^{-1}. Anal. Calcd for $C_{22}H_{19}BrO$: C, 69.66; H, 5.05. Found: C, 69.64; H, 5.10.

6-(1-Pyrene)bromohexane (**13**). $AlCl_3$ (2.1 g, 15.2 mmol) was dissolved in 20 mL of Et_2O in a three-neck round-bottom flask fitted with a reflux condenser. $LiAlH_4$ (15.2 mL of a 1.0 M solution in Et_2O, 15.2 mmol) was then added dropwise, producing a white solid. **12** (2.3 g, 6.1 mmol) was then added dropwise as a solution in CH_2Cl_2, giving an immediate reaction, which caused the solution to boil. After the mixture was stirred for 1 h, the reaction was quenched first by the careful addition of water, followed by 1 M aqueous HCl. The reaction was then washed with aqueous NaCl, and the organic phase was collected and dried over $MgSO_4$. Solvent removal gave the crude product as a yellow solid that was purified by column chromatography

Scheme 2. Synthesis of MMPC **4**

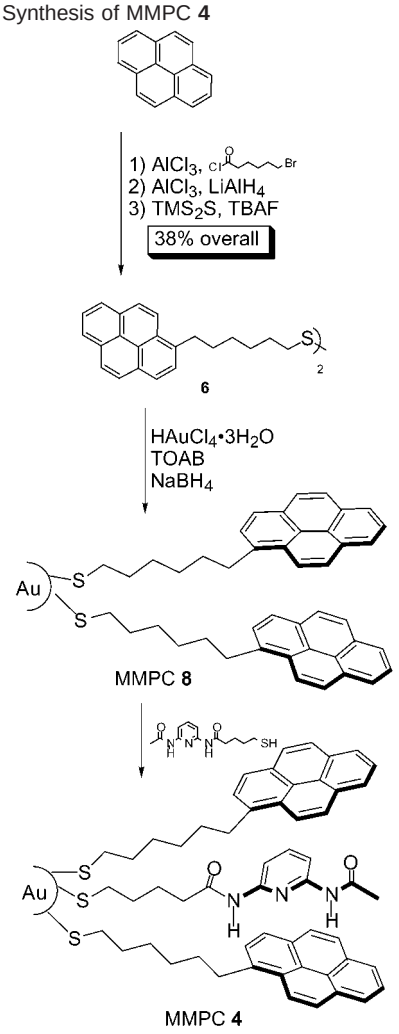

(SiO_2; 1:19 CH_2Cl_2:hexanes) to yield the product as a white solid (2.1 g, 95% yield). ^1H NMR ($CDCl_3$, 200 MHz) δ (ppm) 7.78−8.18 (m, 9H), 3.38 (superimposed triplets, 4H), 1.90 (m, 4H), 1.50 (m, 4H). IR (thin film from CH_2Cl_2 on NaCl plate) ν_{max} 3040, 2922, 2890, 1478, 840 cm^{-1}. Anal. Calcd for $C_{22}H_{21}Br$: C, 72.33; H, 5.74. Found: C, 72.56; H, 5.56.

6-(1-Pyrene)hexanethiol Disulfide (**6**).[27] **13** (250 mg, 0.68 mmol) was dissolved in 20 mL of nondistilled THF in a 50 mL round-bottom flask. Bis-trimethylsilyl sulfide (150 mg, 0.85 mmol, 0.2 mL) was added followed by tetra-*n*-butylammonium fluoride (0.75 mL of a 1.0 M solution in THF, 0.75 mmol). The reaction rapidly changed color to dark green, then slowly to yellow. After the solution was stirred overnight, water was added, and the reaction was stirred an additional 2 h. The light yellow solution was then washed once with aqueous NaCl, and the organic phase was collected and dried over $MgSO_4$. Solvent removal gave the crude product as a yellow solid that was purified by column chromatography (SiO_2; 1:9 CH_2Cl_2:hexanes) to yield the product as a white solid (190 mg, 86% yield). ^1H NMR ($CDCl_3$, 200 MHz) δ (ppm) 7.82−8.27 (m, 9H), 3.31 (t, 2H, J = 7.94 Hz), 2.65 (t, 2H, J = 7.22 Hz), 1.75 (m, 4H), 1.47 (m, 4H). IR (thin film from CH_2Cl_2 on NaCl plate) ν_{max} 2995, 2835, 1090, 835 cm^{-1}. EI-HRMS: (*m*/*z*) 634 (parent ion), 317, 215, 202.

MMPC 8. $HAuCl_4 \cdot 3H_2O$ (470 mg, 1.2 mmol) was dissolved in 150 mL of deionized H_2O in a 500 mL round-bottom flask, giving a golden yellow solution. Tetra-*n*-octylammonium bromide (1.3 g, 2.4 mmol) and 150 mL of toluene were then added and the mixture stirred. After

(27) Hu, J.; Fox, M. A. *J. Org. Chem.* **1999**, *64*, 4959−4961.

15 min, the organic layer had become dark red and the aqueous phase colorless. Disulfide **6** (460 mg, 0.72 mmol) was then added, and the reaction stirred for 30 min to ensure complete dissolution of the disulfide. $NaBH_4$ (500 mg, 10 mmol) was next added dropwise as a solution in 5 mL of H_2O, causing an immediate color change to dark brown and the evolution of gas. After 3 h, the organic phase was collected and the solvent removed. The resulting residue was dissolved in ca. 20 mL of toluene and 200 mL of acetonitrile was then added to precipitate the colloid. When precipitation was complete, the product was collected by filtration, but repeated precipitation was unable to fully remove unused disulfide. Further purification was possible by stirring the colloid for several nights as a suspension in acetonitrile. A final toluene/acetonitrile precipitation step was used to collect the purified colloid. ^{1}H NMR ($CDCl_3$, 200 MHz) δ (ppm) 7.37 (vbs), 2.57 (bs), 1.55 (bs). IR (thin film from CH_2Cl_2 on NaCl plate) ν_{max} 3080, 2920, 2850, 1525, 1395, 1275, 850, 720 cm^{-1}. UV−vis (CH_2Cl_2 solution) λ_{max} 248, 255, 272, 285, 323, 337, 350, 520 (shoulder) nm.

MMPC 4. MMPC **8** (400 mg) and **5** (40 mg, 0.15 mmol) were dissolved in 30 mL of CH_2Cl_2 in a 50 mL round-bottom flask. The resulting dark brown solution was purged with Ar for 30 min, then allowed to stir for 2 days under Ar. The CH_2Cl_2 was removed, and the resulting brown solid was stirred overnight as a suspension in CH_3CN and filtered. This process was repeated as necessary, typically four or five nights, to completely remove unbound thiols as detected by either TLC or NMR. ^{1}H NMR ($CDCl_3$, 200 MHz) δ (ppm) 7.45 (vbs), 5.15 (bs), 2.04 (s), 1.67 (s), 1.24 (s), 0.85 (bm). IR (thin film from CH_2Cl_2 on NaCl plate) ν_{max} 3350, 3290, 3080, 2920, 2850, 1650, 1580, 1450, 1275, 820, 722 cm^{-1}. UV−vis (CH_2Cl_2 solution) λ_{max} 246, 268, 280, 332, 348, 520 (shoulder) nm.

Acknowledgment. This research was supported by the National Science Foundation (CHE-9905492 and MRSEC instrumentation) and the National Institutes of Health (GM 59249). V.M.R. acknowledges support from the Alfred P. Sloan Foundation, Research Corporation, and the Camille and Henry Dreyfus Foundation. A.K.B. would like to thank the American Chemical Society, Division of Organic Chemistry and Boehringer Ingelheim Pharmaceuticals, Inc. for receipt of a 2000−2001 Graduate Fellowship.

Supporting Information Available: Characterization data for all intermediates and MMPCs (PDF). This material is available free of charge via the Internet at http://pubs.acs.org.

JA016894K